Electrochemical ozone sensors: A miniaturised alternative for ozone measurements in laboratory experiments and air-quality monitoring

Xiaobing Pang [a,b,*], Marvin D. Shaw [a,c], Alastair C. Lewis [a,c,*], Lucy J. Carpenter [a], Tanya Batchellier [a]

[a] Wolfson Atmospheric Chemistry Laboratories, Department of Chemistry, University of York, York, YO10 5DD, UK
[b] Key Laboratory for Aerosol-Cloud-Precipitation of China Meteorological Administration, Nanjing University of Information Science and Technology, Nanjing, 210044, China
[c] National Centre for Atmospheric Science, University of York, York, YO10 5DD, UK

ABSTRACT

Ozone (O_3) measurements are a critical component of air quality management and many atmospheric chemistry laboratory experiments. Conventional ozone monitoring devices based on UV absorption are relatively cumbersome and expensive, and have a relative high power consumption that limits their use to fixed sites. In this study electrochemical O_3 sensors (OXB421, Alphasense) were used in a miniaturised O_3 measurement device combined with LabJack and Labview data acquisition (DAQ). The device required a power supply of 5 V direct current (VDC) with a total power consumption of approximately 5 W. Total weight was less than 0.5 kg, low enough for portable *in situ* field deployment. The electrochemical O_3 sensors produced a voltage signal positively proportional to O_3 concentrations over the range of 5 ppb–10 ppm. There was excellent agreement between the performances of two O_3 sensors with a good linear coefficient ($R^2 = 0.9995$). The influences of relative humidity (RH) and gas sample flow rate on sensor calibrations and sensitivities have been investigated separately. Coincident calibration curves indicate that sensor performances were almost identical even at different RHs and flow rates after a re-zeroing process to offset the sensor baseline drifts. Rapid RH changes ($\sim$20%/min) generate significant and instant changes in sensor signal, and the sensors consistently take up to 40 min to recover their original values after such a rapid RH change. In contrast, slow RH changes ($\sim$0.1%/min) had little effect on sensor response. To test the performance of the miniaturised O_3 device for real-world applications, the O_3 sensors were employed for (i) laboratory experiments to measure O_3 loss by seawater uptake and (ii) air quality monitoring over an 18-day period. It was found that ozone uptake by seawater was linear to the volume of linoleic acid on a sea surface microlayer and the calculated uptake coefficients based on sensor measurements were close to those from previous studies. For the 18-day period of air quality monitoring the corrected data from the O_3 sensor was in a good agreement with those obtained by reference UV O_3 analyser with an r^2 of 0.83 ($n = 8502$). The novelty of this study is that the electrochemical O_3 sensor was comprehensively investigated in O_3 measurements in both laboratory and ambient air quality monitoring and it can to be a miniaturised alternative for conventional O_3 monitoring devices due to its low cost, low power-consumption, portable and simple-conduction properties.

1. Introduction

Ozone sensors are a technology for O_3 detection that are characterised as being compact in size, low cost, low power and fast response. Most commercially available O_3 sensors use either electrochemical sensing principles or are based on semiconductor O_3 sensors. Such O_3 sensors have in principle sufficient sensitivity to be used in the ppb-range as air quality monitors for outdoor air. The low cost nature of O_3 sensors allows them to be potentially deployed in denser networks of measurement, giving improved insight into human exposure. The low cost of sensors, as compared to traditional instruments, can enable a democratization of air quality observations to the general public and raise environmental awareness of air pollution. O_3 measurement is a critical component of not only air quality management but is also a key

* Corresponding authors at: Wolfson Atmospheric Chemistry Laboratories, Department of Chemistry, University of York, York, YO10 5DD, UK.
E-mail addresses: pangxbyuanj@gmail.com, pangxbyuanj@163.com (X. Pang), ally.lewis@york.ac.uk (A.C. Lewis).

part of laboratory experiments in atmospheric chemistry, for example for the study of the interaction of O_3 with various chemicals including on surfaces. To date, the most commonly employed ozone monitoring devices are photometric ozone instruments based on UV absorbance, which require high sampling gas flow (>1 L/min), are high power-consuming, cumbersome and expensive. On some occasions the measurement of gaseous ozone using conventional instrumentation is impossible, for example during smog chamber simulation experiments where gas volumes are limited or cannot be supplied at flow rates high enough for UV instruments. Under such situations several optical methods including cavity ring-down spectroscopy (CRDS) and differential optical absorption spectroscopy (DOAS) can be employed for *in situ* ozone detection [1,2]. However, these optical methods are highly specialized making them unavailable for many laboratories. Air quality monitoring networks also typically use expensive measurement apparatus, usually in a fixed location, and equipped with a permanent ac power supply and other secure facilities. However, the densities of monitoring networks are relatively sparse for specific research such as personal exposure studies or mapping the fine scale spatial distribution of O_3 concentrations across large and complex cities [3,4].

The recent development of miniaturised gas sensor technologies has created the opportunity to develop cheap and simple techniques for the rapid and sensitive *in situ* O_3 measurement without requirement for high gaseous sample flows in laboratory experiments. Compared with above three conventional O_3 monitoring devices O_3 sensors are much lower in cost (<$200), have lower power consumption (<5 W), are lighter in weight (<10 g), whilst maintaining high time-resolution (1 s) of measurement. For air quality monitoring, gas sensor techniques can potentially realise low cost flexible networks at high spatial resolution, reducing air pollution monitoring costs and increasing coverage especially in remote areas [5,6]. Cost-efficient ozone sensors based on gas-sensitive semiconducting oxide technology were previously deployed for accurate surface O_3 monitoring in a high spatial density in a valley of New Zealand [3]. Several portable gas sensors was employed to capture the spatial variability of traffic-related air pollution such as O_3 and NO_2 [4]. Due to their portability and low power consumption, other atmospheric gas sensors have been utilised on several specific occasions such as during aircraft measurements and for personal exposure determinations. A custom, compact, laser-based methane sensor was developed and coupled to an unmanned aerial vehicle, which was flown around a compressor station to quantify fugitive methane emissions [7]. A black carbon sensor combined with a smartphone was employed to continuously measure black carbon levels to estimate personal exposures related to residential air pollution and commuting based on personal location and physical activity level [8]. Electrochemical sensors have been employed for monitoring ambient air quality on several occasions [9–14]. However, there are a wide range of sensor types and brands and the sensor performances are still not well understood or comprehensively tested [12,15].

In this paper miniaturised electrochemical O_3 sensors were used in a portable O_3 measurement device combined with an "in house" data acquisition system. The O_3 sensor device was evaluated at low gaseous sample flow rates (0.3 L/min) to study O_3 uptake coefficients of the seawater surface microlayer with polyunsaturated fatty acids, which react with ozone. The performances of the O_3 sensor for ambient air quality monitoring was also investigated during an 18-day summer field campaign, where the sensor response was compared with a reference UV O_3 monitor (Thermo 49C UV absorption ozone analyser). The influences of relative humidity (RH) and gas flow rate on sensor performances were investigated independently.

2. Experimental

2.1. Commercial O_3 sensors

Two commercial O_3 sensors (Model OX-B421), their support circuit boards and their gas hoods for individual sensor were purchased from Alphasense, UK. The O_3 sensor was integrated with the support circuit board and gas hood, where the circuit board, which is pre-configured for each sensor and provides a low noise and high resolution signal output, through its electrodes. The gas hood is sealed on the cap of sensor to assist sample gas contact with the diffusion barrier allowing ozone diffusion into the electrolyte. In laboratory experiment two sensors were used to measure the O_3 mixing ratios at inlet and outlet of a flow reactor, respectively (Fig. 1(b)). During air quality monitoring two sensors were compared with each other to evaluate differences between devices (Fig. 1(c)). The O_3 sensors are based on electrochemical reactions that take place within the sensor between O_3 and a certain electrolyte. The specifications of the electrochemical sensor are listed in Table 1. The O_3 sensor has a working electrode (WE), a reference electrode (RE) and a counter electrode [10]. The RE response is used to compensate for drifting of the offset zero voltage. The resulting voltage between WE and RE are the signal current from the target gas measurement. The circuit board is preconfigured for each individual sensor with fixed zero and electronic gain (sensitivity, unit: voltage/ppb) and also provides a buffered voltage output from both the WE and RE with lowest noise. The gas concentrations measured by such electrochemical sensors can be calculated according to the following equation.

$$\text{gas concentration (ppb)} = \frac{(WE_i - WE_0) - (RE_i - RE_0)}{\text{Sensitivity}} \tag{E1}$$

In the above equation WE_0 and RE_0 are the offset voltages of the WE and RE, respectively, which are used to compensate for the sensor specific offset voltage of each sensor. These values were determined against dry zero air. WE_i and RE_i are the output voltages of the WE and RE during the measurement of the gaseous sample.

The sample gas temperature, pressure and humidity were measured in line using a LM35 temperature sensor (Texas Instruments), MPX4200A absolute pressure sensor (Freescale Ltd.) and an HIH-4000-001 humidity probe (Honeywell), respectively. During the analysis periods, in line gas temperature and pressure were consistent, $20.2 \pm 0.7\,^\circ C$, 1.0003 ± 0.0009 bar respectively, minimising their effects upon the sensors.

2.2. Data acquisition

All sensors were connected through LabJack data-acquisition (DAQ) device (U6 Series, LabJack Corporation, USA) to our Lab-VIEW in-house designed DAQ software. Through this software we monitor the output voltage of the sensor and convert the voltage signals into gas concentrations. The data acquisition rate was 1 Hz (averaged to 1 min intervals for laboratory measurement and 5 min intervals for ambient O_3 monitoring, respectively).

The control software for the DAQ system was written using LabVIEW software (LabVIEW 2012, National Instrument, USA). The host PC displays the user interface including four tabs such as sensor control, sensor data, diagnostic data etc., by which the user can specify the data acquisition rate, the file-path of data saving, auto-zeroing the voltage of WE and RE, and the sensitivity setting (Voltage/ppb). Once deployed, the control software runs autonomously and the O_3 concentrations are displayed continuously on the tab of sensor data. All data are saved automatically during the sensor working period including O_3 concentration (ppb), voltages of WE and RE, RH, temperature, air pressure, respectively.
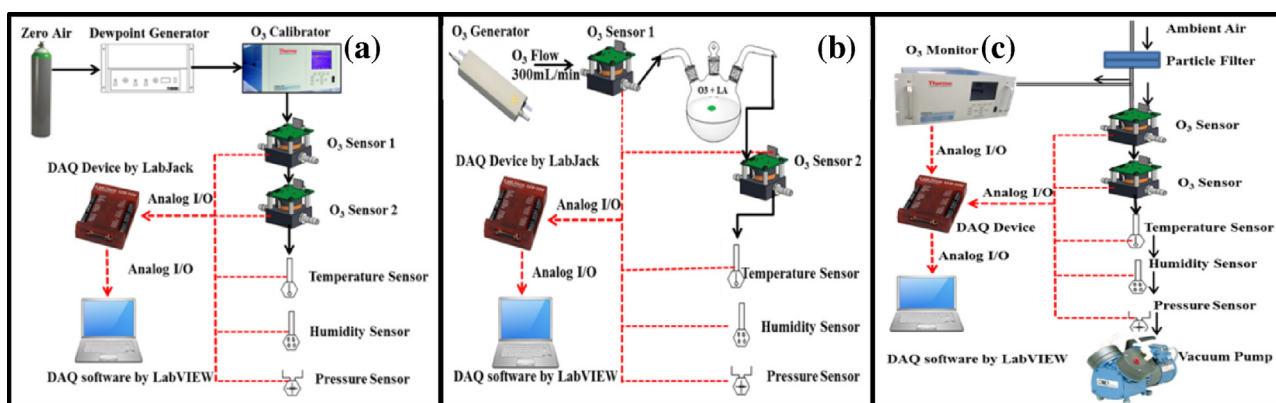
Fig. 1. Schematic diagrams of the experimental setup for O_3 sensor performance tests. (a) calibration setup for O_3 sensors, (b) O_3 uptake by seawater with linoleic acid (LA) on its surface, (c) ambient O_3 measurement by two O_3 sensors.

Data files are saved in a LabVIEW format which can be easily converted to .txt or .csv data for future use.

2.3. Calibration

All O_3 sensors were initially zeroed using zero grate air All O3 sensors were initially zeroed using zero grade air, which is produced by mixing pure oxygen (20%) and pure nitrogen (80%) and provided by BOC, UK and then calibrated under a series of O_3 standard gases to ensure their accurate sensitivities. The experimental setup for the calibration is schematically shown in Fig. 1(a). A certified multi-gas calibrator (S6100, Environics, US) with an internal O_3 generator was used for O_3 sensor calibration. 10 ppb–1000 ppb O_3 standard gases were generated for the calibration since this range of O3 mixing ratios cover O_3 concentration in ambient air and laboratory experiment in this study. For O_3, the reference instrument was a Thermo Environmental Instruments (TEI) 49C UV absorption ozone analyser which is a United States Environmental Protection Agency (USEPA) equivalent method. Calibration of the instrument was carried out using a TEI Primary Ozone standard, which itself is certified yearly by the UK National Physical Laboratory (NPL). The instrument provided minute averaged data.

During calibration the observed raw concentrations on exposure to the O_3 standard gas (defined as C_{raw}) are based on the initial sensitivities (defined as $S_{initial}$), which is provided by the manufacturer according to Eq. (E1). The C_{raw} is a little different from the true concentration (defined as C_{true}), which was directly read from the O_3 calibrator. Through the (E1) equation the calibrated sensitivity of sensor (defined as $S_{calibrated}$) can be calculated and obtained based on Eq. (E2).

$$S_{calibrated} = \left(\frac{C_{raw}}{C_{true}} \right) * S_{initial} \qquad (E2)$$

The $S_{calibrated}$ was then input into the LabVIEW DAQ software to replace the $S_{initial}$ and the O_3 sensor then reports data calibrated to the reference gas. All O_3 sensors were subsequently zeroed at the flow of zero grade air, which is produced by mixing pure oxygen (20%) and pure nitrogen (80%) and provided by BOC, UK, and calibrated weekly. To investigate the effect of RH on sensor performance a dew-point generator (DG3, Michell Instruments, UK)

was employed to produce various RH sample gases in the range of 15%–85% RH, which covers the main RHs in ambient air.

2.4. Effect of RH and flow rate on sensor calibrations and sensitivities

Relative humidity (RH) and flow rate are two of essential factors for sensor performance that can cause variations in sensor sensitivity, sensor gain and sensor baseline [16]. In this study the sensor calibrations were conducted on various RHs (15%, 45%, 60%, 75% and 85%, respectively) and the flow rates of gas sample (300, 500, 700, and 1000 mL/min, respectively) and the variations of sensor sensitivity were investigated simultaneously. The O_3 sensors were firstly calibrated with O_3 standard gases at eight mixing ratios including 0, 60, 120, 180, 240, 320, 480, and 960 ppb, respectively, which were produced by the O_3 generator.

2.5. Sensor applications: O_3 uptake and air quality monitoring

To evaluate the sensor performance, the O_3 sensors were applied to quantitatively determine O_3 in both laboratory experiments and air quality monitoring separately. In the laboratory, O_3 sensors were applied to measure ozone uptake by seawater through the determination of O_3 at the inlet and outlet of a reaction vessel, where O_3 (210 ppb at 300 mL/min) reacted heterogeneously with linoleic acid at the surface microlayer of seawater (200 mL). The O_3 concentration difference between two positions in the reaction vessel was assumed to be exclusively due to O_3 loss through surface reaction with linoleic acid, which can be utilised to calculate the O_3 uptake coefficient. The detailed experimental setup is schematically shown in Fig. 1(b) and the experimental conditions for O_3 uptake experiment are listed in Table 2.

For air quality monitoring an O_3 sensor was employed to monitor ambient O_3 over an 18-day period (from 7th to 25th August 2015) alongside reference measurements. The sampling site is located in the campus of University of York, UK and the air sample was drawn from a building roof (10 m above ground level). Ambient air was introduced to the gas hood of the O_3 sensor from the main sample inlet using a stainless steel diaphragm metal bellows pump (Senior Aerospace, MB302) at a flow rate of 1 L/min. The air sample flow passed simultaneously into a UV photometric O_3 anal-

Table 1
Specifications of O_3 sensor employed in this study.

Sensor model	Size (L × W × H)[a]	Weight (g)[a]	Power supply (VDC)	Linear Range (ppm)	Noise (ppb)
O_3, OX-B421	4.5 × 4.0 × 4.0 cm	100	5	0–20	15

[a] The size and the weight are measured based on the sensor, individual sensor board, gas hood, and mounting kits in a whole.

Table 2
Experimental conditions for experiments measuring O_3 uptake by seawater and for air quality monitoring.

Experiment	Flow Rate (L/min)	RH (average) (%)	Temp. (average) (°C)	Time Resolution (min)
O_3 uptake	0.3	70–80 (76.2)	20–22 (21.2)	1
air O_3 monitoring	1.0	40–90 (59.6)	12–26 (17.1)	5

yser (Model 49C, Thermo Electron Corporation, USA) for reference measurement. Sensor and reference measurement data were averaged to 5 min intervals and evaluated over the 18-day period. The detailed experimental setup is schematically shown in Fig. 1(c) and the experimental conditions are listed in Table 2.

The selectivity of this electrochemical O_3 sensor can be affected by cross interferences from other gases including NO_2, NO, and RH in ambient air when the O_3 sensor was employed in air quality monitoring [15]. The interferences have observable effects on the WE voltage but no influences in AE voltage of the sensor during the experiments. The corrected WE voltage of O_3 sensor during air quality monitoring can be calculated by the following Eq. (E3).

$$WE_{correct} = WE_{initial} - [NO_2] \times NO_{2response} - [NO] \times NO_{response} - RH$$
$$\times RH_{response} \qquad (E3)$$

In the above equation $WE_{correct}$ and $WE_{initial}$ are the corrected WE voltage and initial WE voltage of O_3 sensor. $NO_{2response}$, $NO_{response}$, and $RH_{response}$, are the WE responses ($mV\,ppb^{-1}$) due to the presence of NO_2, NO, and RH in ambient air, respectively, which were calculated and listed in our previous study [15]. During the 18-day period of air quality monitoring the ambient concentrations of NO_2 and NO were monitored by a single channel chemiluminescence instrument (Air Quality Design Inc., USA) [17]. The corrected WE voltages obtained from E3 were employed to calculate actual O_3 concentrations through Eq. (E2).

3. Results and discussions

3.1. Relationship between output voltage of O_3 sensor and O_3 concentration

The operational theory of electrochemical gas sensors is that the target gas diffuses into the sensor through a capillary diffusion barrier to the working electrode where it is oxidized or reduced [16]. This electrochemical reaction results in an electric current that passes through the external circuit. The output voltage from the sensor is linearly proportional to the gas concentration in a certain range. In this study the output voltages of the O_3 sensor were
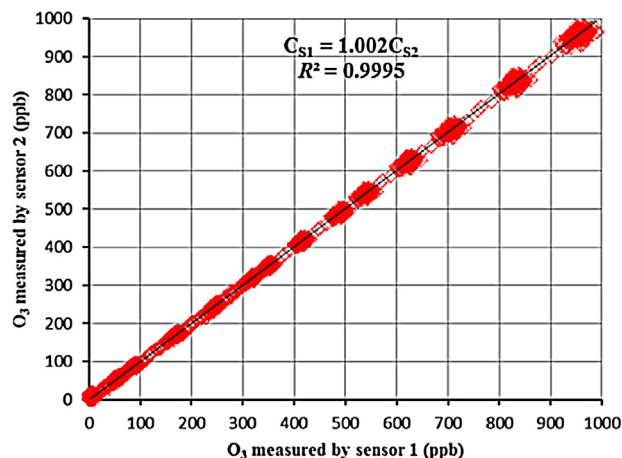

Fig. 3. Comparison between sensor 1 and sensor 2 for O_3 measurements from 0 to 998 ppb. A good agreement is found between two O_3 sensors with a linear coefficient ($R^2 = 0.9995$, $n = 6257$). Experimental conditions: RH: $60 \pm 5\%$, flow rate of sample gas: 300 mL/min, temperature: 20 °C.

observed to linearly increase from 43 mV to 2500 mV as O_3 concentration increased from 100 ppb to 10 ppm (Fig. 2a). A significant linear relationship with a coefficient (R^2) of 0.9998 can be observed between the sensor output voltage and O_3 concentration (Fig. 2b).

3.2. Inter-comparison of sensor performance

In this study two O_3 sensors were used to measure O_3 concentrations at the inlet and outlet of a reaction vessel to measure the ozone loss. It is crucial that, once calibrated, the two sensors can perform consistently with respect to one another. Two O_3 sensors were utilised to simultaneously detect a series of O_3 standard gases from 4.0 ppb to 975 ppb. The performances of two sensors to O_3 standard gases were compared and shown in Fig. 3. It can be seen that the performances of two sensors correlate well with a linear coefficient (R^2) of 0.9995 ($n = 3040$) when O_3 mixing ratios varied in the range of 10 ppb–1000 ppb. It should be noted that the limit of detection of the sensor is 5 ppb, which can explain why the perfor-
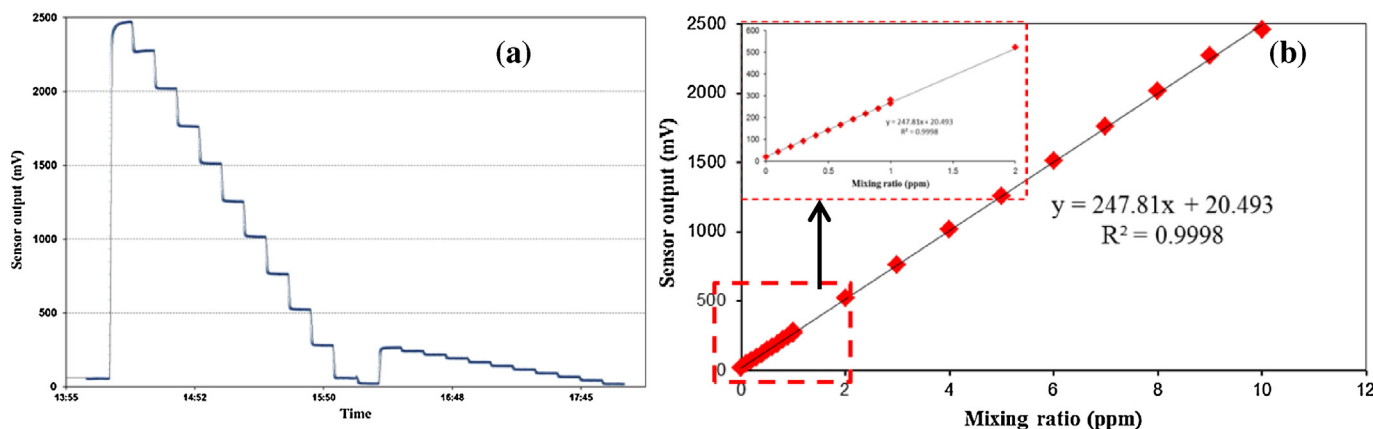

Fig. 2. (a): Relationship of O_3 sensor output voltage and O_3 concentration varying from 100 ppb to 10 ppm; (b): A good linear relationship can be observed between sensor output voltage and O_3 concentrations with a linear coefficient (R^2) of 0.9998. Experimental conditions: RH: $60 \pm 5\%$, flow rate of sample gas: 300 mL/min, temperature: 20 °C.
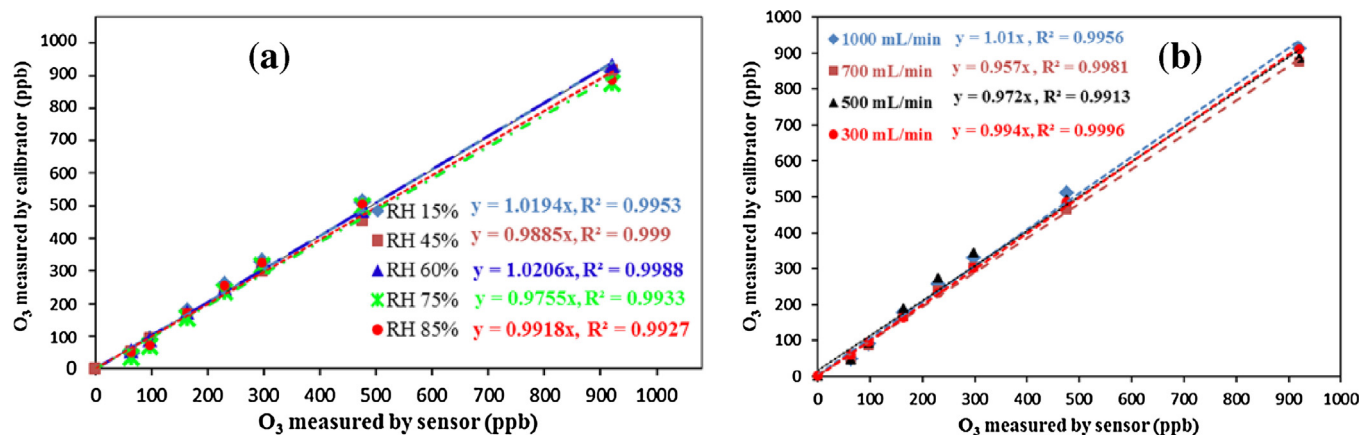
Fig. 4. (a) Sensor calibrations under different relative humidity (RH). Experimental conditions: flow rate of sample gas: 500 mL/min, temperature: 20 °C; (b) Sensor calibrations under various gas flow rates. Experimental conditions: RH: 60 ± 5%, temperature: 20 °C.

mances of two sensors were inconsistent to the gas samples with O_3 mixing ratios below to 5 ppb.

3.3. Effects of relative humidity and flow rate on calibrations

The O_3 sensors had been calibrated under five different RHs including 15%, 45%, 60%, 75% and 85%, respectively. The sensor baseline drifted after each RH change and the sensor was zeroed to offset the drift of baseline before the calibration at each RH. The sensor was then calibrated under eight different O_3 mixing ratios. A calibration curve at each RH was set up between the values of O_3 concentration obtained by the sensor and the reference values provided by the O_3 generator. Those calibration curves under various RHs are almost coincident each other (Fig. 4a), which indicates the sensor performances were almost identical at different RHs. The maximum derivation (4.6%) of the slopes of calibration curves, which was found between those of RH 60% and RH 75%, may be due to the random variability of measurements. This result demonstrates that the performances of the O_3 sensor can be consistent at different RHs after a zeroing process to offset the baseline drifts due to RH change. Accuracies and precisions of sensor performances were listed in Table 3 at various RHs to different O_3 mixing ratios. The accuracies at most measurements are below to 15% and the precisions are lower than 5%, which indicates the performances of O_3 sensor are satisfactory in deployment.

However, the sensor performance is slightly different if the sensor was not zeroed to offset the baseline drift due to each rapid RH change. As Fig. 5(a) shows the sensor reading dramatically decreases to approximately 0 ppb from 70 ppb at the beginning of each rapid RH decrease at a rate of −20%/min and then gradually recovers to their initial value (70 ppb) after 40–60 min. In contrast if the RH rapidly increases at 20%/min, the sensor signal rapidly jumps to 300 ppb from 70 ppb and then gradually drops down to the 80–100 ppb after a balance period of 15–40 min. If the RH changes slowly, the situation of sensor response is quite different. As Fig. 5(b) shows, the sensor signals remain stable in the range of 65–75 ppb when the RH slowly decreased from 60% to 30% over six hours at a rate of 0.1%/min. As the RH further rapidly decreased from 30% to 5% in 15 min, the sensor reading significantly reduced to 0 ppb from 75 ppb and then gradually recovered to 70 ppb in 15 min at the stable RH (5%). These experiments imply that sensor performance is relatively consistent if the environmental RH varies slowly. So the influence of RH on sensor performance can be ignored if the sensor was employed for experimental gaseous samples at stable RH or for air quality monitoring under a stable weather con-

dition with slower RH ambient changes [18]. The relation between RH variation and sensor recovery time is unclear based on above experimental phenomenon.

The voltage outputs of both WE and RE were investigated during a process of RH increases in a gas sample containing the consistent O_3 mixing ratios (Fig. 6). The voltage outputs of WE and RE showed the same varying tendency, i.e. both initially increased with the increased RH and then gradually stabilised at higher values (Fig. 6). The WE voltages increased dramatically during the initial minutes of the RH change, which can explain why the O_3 sensor reading sharply rose at the beginning of the RH change. The final stabilised voltages from WE and RE can explain why the sensor reading recovered to a stable level after a 40 min period (Fig. 5a). The RH was observed to have a positive linear relationship with the voltages from WE and RE (Fig. 6c) but the slope of the calibration curve between WE and RH was a little higher than that between RE and RH. As the increase of WE voltage is higher than that of the RE voltage (Fig. 6c) the O_3 concentrations calculated by the Eq. (E1) will be higher. This result can explain why the O_3 sensor data were sometimes greater than the initial data after a RH increase in Fig. 5a.

The effect of gas flow rate on O_3 sensor performance was investigated under four flow rates including 300 mL/min, 500 mL/min, 700 mL/min and 1000 mL/min, respectively. Calibrations were conducted under the four flow rates and a series of calibration curves were obtained and shown in Fig. 4b. The calibration curves indicate that the sensor data are nearly equal to those data from O_3 calibrator under the four flow rates with their slopes approaching unity varying between 0.972 to 1.01. Therefore, it can be concluded that the flow rate of sample gas has little influence on the O_3 sensor performances within this range.

3.4. Effects of relative humidity and flow rate on sensitivity

According to Eq. (E1), sensor measurements are controlled by both the sensitivity and output voltage. The effects of RH, flow rate and O_3 concentration on sensor sensitivity were separately studied. As Fig. 7(a) shows that sensor sensitivities are constant in the RH range of 15%–60% and decrease gradually as the RH further increases to 85%, at which point sensor sensitivity is equal to the 80% of those at the RH of 15%. As shown in Fig. 7(b), the sensor sensitivities were nearly stable over the whole concentration range at RHs of 85% and 75% whilst at RHs of 30% and 45% the sensitivities were stable in the range of 60–300 ppb but decreased by about 8% with the further increase of O_3 to 990 ppb. As Fig. 7(c) implies, gas flow rate has a clear negative correlation on the sensor sen-

Table 3
Accuracy and precision of O$_3$ sensor at various RHs to different O$_3$ mixing ratios.

Refer. Value(ppb)[a]	15% (RH)		45%		60%		75%		85%	
	Accuracy (%)[b]	Precision(%)[c]	Accuracy	Precision	Accuracy	Precision	Accuracy	Precision	Accuracy	Precision
64	−14	5	9	4	7	5	−23	5	15	4
97	−7	4	1	3	1	4	−15	6	2	4
164	7	2	5	4	3	4	−11	5	11	3
230	11	2	7	2	5	3	−5	4	6	1
298	10	1	9	1	8	2	−2	2	3	2
476	7	1	11	1	7	1	2	1	1	2
921	−1	1	0	0	2	1	−6	1	1	1

[a] Reference values are the O$_3$ mixing ratios provided by the O$_3$ generator.
[b] Accuracy is calculated by the equation of (Sensor value − Refer. value)/Refer. value * 100%. Sensor value are the average of over 100 data.
[c] Precision is calculated by the equation of (Standard derivation/Sensor value * 100%).
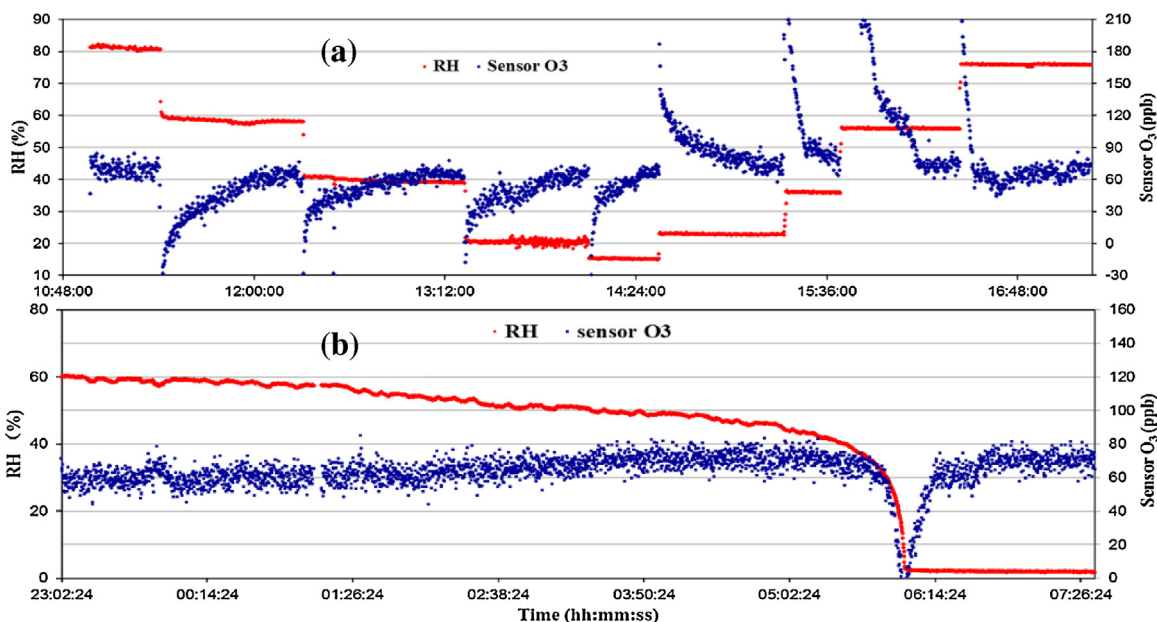

Fig. 5. Humidity effects on O$_3$ measurement by the sensors. (a): O$_3$ sensor responses to rapid RH changes where RH decreased from 80% to 15% and then increased from15% to 75%. (b) O$_3$ sensor responses to slow RH changes where RH gradually decreased from 60% to 30% in 7 h and further decreased from 30% to 4% in 5 min. Experimental conditions: O$_3$ concentration in gaseous flow is 70 ppb and the gaseous flow rate is 300 mL/min.

sitivity, which decreases from 8.8×10^{-4} V/ppb at 300 mL/min to 5.2×10^{-4} V/ppb at 1000 mL/min with a pronounced decrease up to 40%.

As mentioned above, the voltages of both the WE and the RE increase with increasing RH for the gas samples in the presence of same O$_3$ mixing ratio (Fig. 6). The elevated output voltage due to the RH increases is actually the offset voltage rather than signal voltage from O$_3$ measurement. So lower signal voltage swill be output after the O$_3$ sensor is zeroed to balance the higher offset voltages due to a RH increase. As a result, to reach the same and accurate values the sensitivity of the sensor accordingly decreases due to the lower signal output from the sensor based on Eq. (E1). The same mechanism can be used to explain why flow rate has a negative effect on the sensor sensitivity in this study.

3.5. O$_3$ sensors in laboratory experiments and air quality monitoring

To validate and evaluate the performance of O$_3$ sensors in both laboratory and field employments, we evaluated the O$_3$ sensors through the sensor application to study the ozone uptake by unsaturated organic acid on seawater in laboratory and to monitor ambient O$_3$ in a field campaign. The schematics of the two experimental setups are shown in Fig. 1(b) and (c).

Uptake of ozone by unsaturated fatty acids on microlayer in seawater is a crucial process affecting the global ozone budget and has recently drawn extensive research attention[1,19,20]. In the ozone uptake experiment two ozone sensors were used to measure the initial ozone concentration at the inlet location of reaction vessel and the final O$_3$ concentration at the vessel outlet. The difference between two sensor measurements is the O$_3$ loss by the seawater uptake. Ozone sensor performance was compared with the reference instrument and both data are consistent, which is shown in Fig. 8(a). We successively measured O$_3$ concentrations in the gas flows prior to the inlet of reaction vessel and from the outlet of the reaction vessel containing five artificial seawater samples (200 mL), which were prepared by dissolving sea salt into purified water to 3.5% salt mass concentration, with the additions of with 0.00, 1.25, 2.50, 3.75, and 5.0 μL of added linoleic acid, respectively. The evolution of O$_3$ concentration with respect to time are displayed in Fig. 8(b). The O$_3$ concentration prior to the inlet of reaction vessel immediately (1 min) reached and kept at a stable level of 210 ppb after the ozone generator was turned on. In contrast, the outlet O$_3$ concentrations took longer to reach a stable level since O$_3$ was absorbed by the seawater and reacted with LA in the reaction vessel reaching equilibrium in approximately 20 min. It was observed that the ozone loss was positively proportional to the LA volume on the surface microlayer of seawater from the above experimental
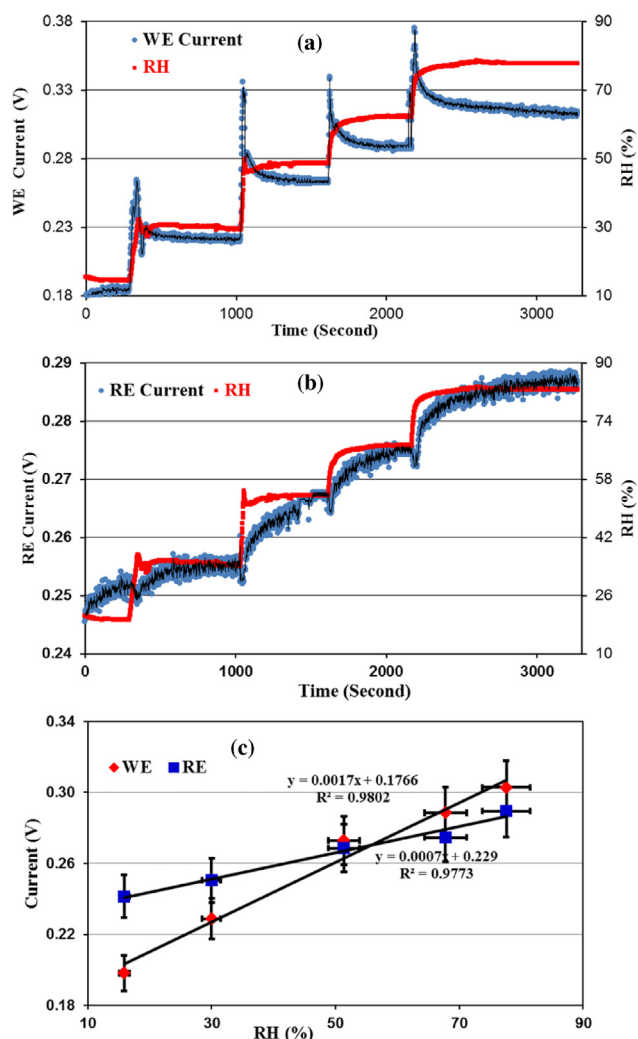
Fig. 6. RH effects of gas sample on WE (panel (a)) and RE (panel (b)) voltage outputs of O_3 sensor and the linear relationships among WE voltage, RE voltage and RH of O_3 gas sample (panel (c)).

Fig. 7. Effects of relative humidity and flow rate of sample gas on O_3 sensor sensitivity. (a) RH effect on O_3 sensor sensitivity with RH varying from 15% to 85%. Experimental conditions: O_3 concentration is 320 ppb and the gas flow rate is 500 mL/min. (b) O_3 sensor sensitivity varies with O_3 mixing ratio at different RHs. Experimental conditions: gas flow rate is 500 mL/min. (c) Effect of flow rate on O_3 sensor sensitivity. Experimental conditions: O_3 mixing ratio is 320 ppb and RH in gas sample is 45%.

result (Fig. 8(c)) since the contact surface of heterogeneous reaction between O_3 and LA on seawater surface increases with the LA concentration.

An O_3 sensor was employed in air quality monitoring and compared with a reference UV photometric O_3 analyser on ambient O_3 measurements over an 18-day period (7/8/2015–25/8/2015). The corrected sensor data are averaged to 5 min intervals and shown in Fig. 9(a) combined with the data of reference measurement. The corrected sensor data are in good agreement with reference data over the whole campaign period with an R^2 of 0.84 ($n = 4768$) (Fig. 9(b)), however, the O_3 sensor measurements overestimated the O_3 concentrations by 20–40% compared with the reference method during peak periods. Average O_3 mixing ratios determined from the sensor and the reference measurements were 24.8 ± 14.5 and 23.6 ± 12.3 ppb, respectively. Average ambient humidity was $59.1 \pm 12.1\%$ ($n = 4768$) during the field campaign, which is within in the optimal RH range for the O_3 sensor performance. Based on the consistent measurements between the O_3 sensor and UV photometric O_3 analyser in the field campaign an unambiguous conclusion was that the O_3 sensor can be employed in air quality monitoring and its performance is in good agreement with conventional UV photometric O_3 analyser.
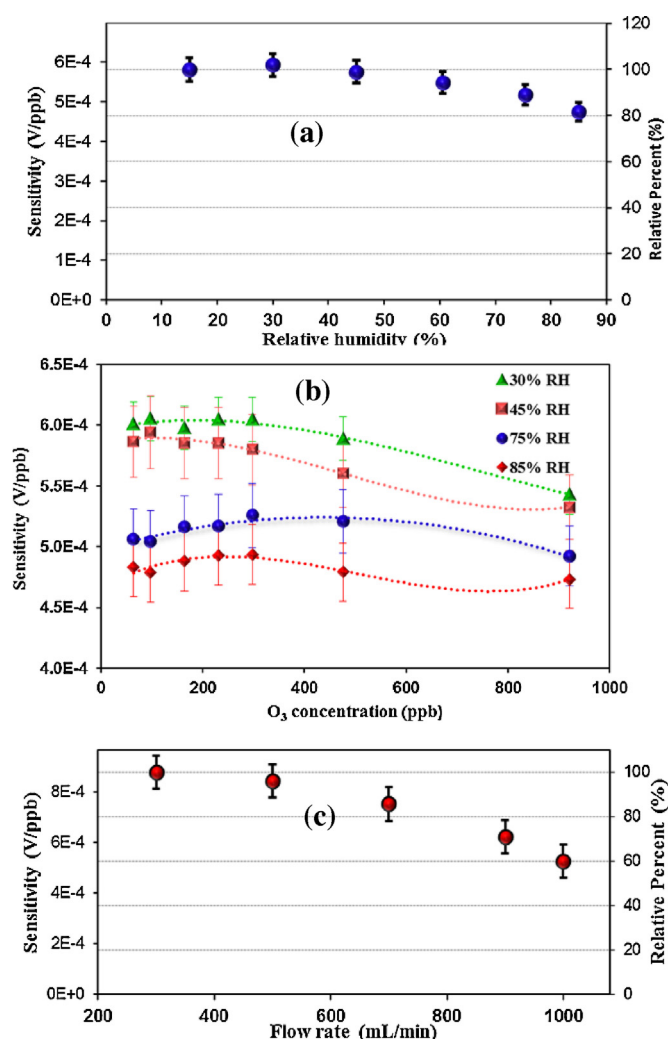
4. Conclusions

In this study the performance of electrochemical O_3 sensors were investigated in both laboratory and ambient air quality monitoring. We show that O_3 sensors can be deployed as a miniaturised alternative for conventional O_3 monitoring devices at lower cost and with low power consumption. The performance of low cost ozone sensors has been characterised under various RHs and sample gas flow rates and then further evaluated in both laboratory experiments and field campaign measurements. All results indicated that the miniaturised O_3 sensor were a suitable alternative for O_3 measurements in both laboratory experiment and air-quality monitoring. The O_3 sensor output voltage was found to have a significant positive linear relationship with O_3 concentration from 5 ppb up to 10 ppm. The performance of two different sensors were strongly correlated to each other after calibration. The sensors performed well only if the sensor was zeroed to the higher offset voltage. The consistent calibration curves for the O_3 sensors working under various RH and flow rates confirm the consistent performance of sensor. However, the voltages of both the WE and RE increase with rapidly increasing RH and flow rates; this causes a
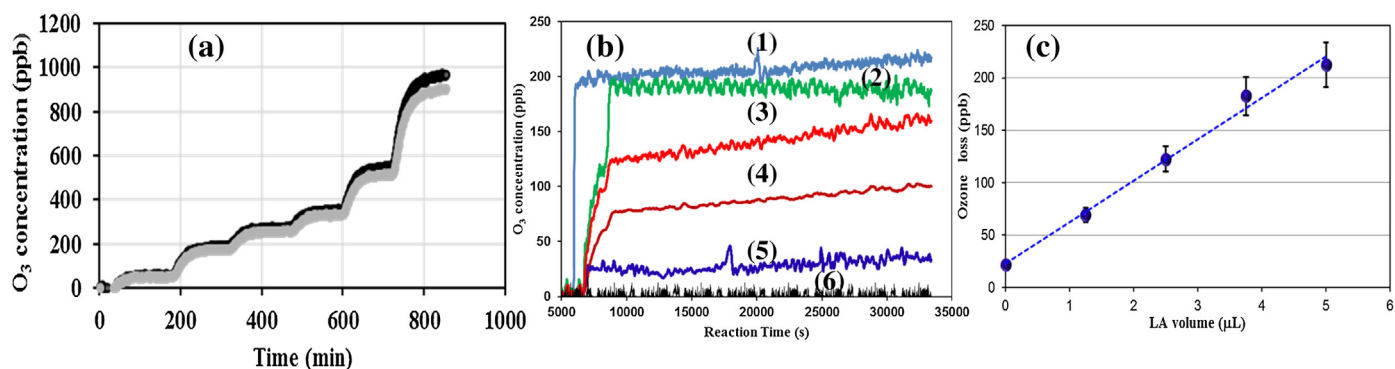
Fig. 8. Evolution of O_3 during an experiment to measure the O_3 uptake by seawater with different volumes of linoleic acid (panel (b)) on its surface. Consistency between ozone sensor (grey line) and reference instrument (black line) (panel (a)). The O_3 evolutions in panel (b) from top to bottom are the O_3 from the outflow of the empty glass vessel reactor (light blue line (1)) and four seawater samples in vessel reactor with 0.00 (green line (2)), 1.25 (red line (3)), 2.50 (brown line (4)), 3.75 (blue line (5)), and 5.0 μL (black line (6)) linoleic acid (LA) on the seawater surface, respectively. Panel (c): the linear relationship between O_3 loss and LA volume on the seawater surface. Experimental conditions: O_3 concentration is 200 ppb and flow rate passing through glass vessel is 300 mL/min. (For interpretation of the references to color in this figure legend, the reader is referred to the web version of this article.)
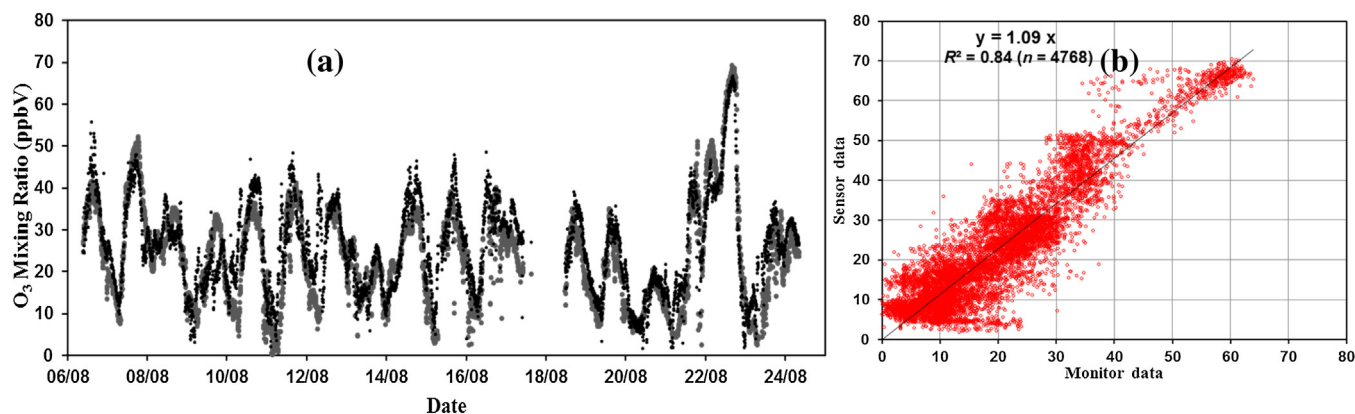

Fig. 9. A time-series comparison between O_3 sensor (black dots) and reference photometric O_3 instrument (grey dots) in air quality monitoring of ambient O_3 (5-min average) during an 18-day (from 7 August 2015 to 25 August 2015) field campaign (panel (a)) and the linear relationship between sensor data and reference instrumental data (panel (b)).

higher offset voltage of the sensor. RH and flow rate have negative influences on the sensor sensitivity since they increase the offset voltage of the sensors thus reducing the sensor output voltage. A caveat, however, has is that the O_3 sensor has a LOD of 5 ppb but that the performance is easily interfered by environmental RH and coexisting compounds. Sensor performance is significantly degraded by any rapid RH variations and the sensor usually takes around 40 min to recover to the initial working status after each rapid RH change. To overcome the RH effects, sensors should be zeroed after each rapid RH variation, or data during the recovering period should be ignored. In a field campaign over an 18-day period, during which RH changed only slowly in ambient air, the O_3 sensor was observed to perform consistently when compared against a reference O_3 analyser. In the foreseeable future the functions of wireless communication and remote control will be added on the sensor DAQ program by LabVIEW software, which will facilitate wider usage of the gas sensors in both research and air quality monitoring. The relation between RH variation and sensor recovery time is unclear and need to be studied further.

References

[1] S. Zhou, L. Gonzalez, A. Leithead, Z. Finewax, R. Thalman, A. Vlasenko, et al., Formation of gas-phase carbonyls from heterogeneous oxidation of polyunsaturated fatty acids at the air–water interface and of the sea surface microlayer, Atmos. Chem. Phys. 14 (2014) 1371–1384.

[2] Y. Sakamoto, A. Yabushita, M. Kawasaki, S. Enami, Direct emission of I2 molecule and IO radical from the heterogeneous reactions of gaseous ozone with aqueous potassium iodide solution, J. Phys. Chem. A 113 (2009) 7707–7713.

[3] M. Bart, D.E. Williams, B. Ainslie, I. McKendry, J. Salmond, S.K. Grange, et al., High density ozone monitoring using gas sensitive semi-conductor sensors in the lower Fraser Valley, British Columbia, Environ. Sci. Technol. 48 (2014) 3970–3977.

[4] L. Deville Cavellin, S. Weichenthal, R. Tack, M.S. Ragettli, A. Smargiassi, M. Hatzopoulou, Investigating the use of portable air pollution sensors to capture the spatial variability of traffic-related air pollution, Environ. Sci. Technol. 50 (2016) 313–320.

[5] W. Tsujita, A. Yoshino, H. Ishida, T. Moriizumi, Gas sensor network for air-pollution monitoring, Sens. Actuators B 110 (2005) 304–311.

[6] M. Lösch, M. Baumbach, A. Schütze, Ozone detection in the ppb-range with improved stability and reduced cross sensitivity, Sens. Actuators B 130 (2008) 367–373.

[7] B.J. Nathan, L.M. Golston, A.S. O'Brien, K. Ross, W.A. Harrison, L. Tao, et al., Near-field characterization of methane emission variability from a compressor station using a model aircraft, Environ. Sci. Technol. 49 (2015) 7896–7903.

[8] M.J. Nieuwenhuijsen, D. Donaire-Gonzalez, I. Rivas, M. de Castro, M. Cirach, G. Hoek, et al., Variability in and agreement between modeled and personal continuously measured black carbon levels using novel smartphone and sensor technologies, Environ. Sci. Technol. 49 (2015) 2977–2982.

[9] T.J. Roberts, C.F. Braban, C. Oppenheimer, R.S. Martin, R.A. Freshwater, D.H. Dawson, et al., Electrochemical sensing of volcanic gases, Chem. Geol. 332–333 (2012) 74–91.

[10] M.I. Mead, O.A.M. Popoola, G.B. Stewart, P. Landshoff, M. Calleja, M. Hayes, et al., The use of electrochemical sensors for monitoring urban air quality in low-cost, high-density networks, Atmos. Environ. 70 (2013) 186–203.

[11] C. Lin, J. Gillespie, M.D. Schuder, W. Duberstein, I.J. Beverland, M.R. Heal, Evaluation and calibration of Aeroqual series 500 portable gas sensors for accurate measurement of ambient ozone and nitrogen dioxide, Atmos. Environ. 100 (2015) 111–116.

[12] N. Masson, R. Piedrahita, M. Hannigan, Quantification method for electrolytic sensors in long-term monitoring of ambient air quality, Sensors 15 (2015) 27283.

[13] I. Heimann, V.B. Bright, M.W. McLeod, M.I. Mead, O.A.M. Popoola, G.B. Stewart, et al., Source attribution of air pollution by spatial scale separation using high spatial density networks of low cost air quality sensors, Atmos. Environ. 113 (2015) 10–19.

[14] L. Spinelle, M. Gerboles, M.G. Villani, M. Aleixandre, F. Bonavitacola, Field calibration of a cluster of low-cost available sensors for air quality monitoring. Part A: ozone and nitrogen dioxide, Sens. Actuators B 215 (2015) 249–257.

[15] A.C. Lewis, J. Lee, P.M. Edwards, M.D. Shaw, M.J. Evans, S.J. Moller, et al., Evaluating the performance of low cost chemical sensors for air pollution research, Faraday Discuss. (2015).

[16] M.L. Hitchman, N.J. Cade, T. Kim Gibbs, N.J.M. Hedley, Study of the factors affecting mass transport in electrochemical gas sensors, Analyst 122 (1997) 1411–1418.

[17] J.D. Lee, S.J. Moller, K.A. Read, A.C. Lewis, L. Mendes, L.J. Carpenter, Year-round measurements of nitrogen oxides and ozone in the tropical North Atlantic marine boundary layer, J. Geophys. Res.: Atmos. 114 (2009) (n/a–n/a).

[18] https://www.niwa.co.nz/education-and-training/schools/resources/climate/plots.

[19] T. Moise, Y. Rudich, Reactive uptake of ozone by aerosol-associated unsaturated fatty acids: kinetics, mechanism, and products, J. Phys. Chem. A 106 (2002) 6469–6476.

[20] T. Thornberry, J.P.D. Abbatt, Heterogeneous reaction of ozone with liquid unsaturated fatty acids: detailed kinetics and gas-phase product studies, Phys. Chem. Chem. Phys. 6 (2004) 84–93.

Biographies

Xiaobing Pang is a research fellow in the Wolfson Atmospheric Chemistry Laboratories, Department of Chemistry, University of York, UK. He obtained his Ph. D. on environmental science from the University of Chinese Academy of Sciences in 2007. His research interests focus on the development of state-of-art techniques for atmospheric compositions including microfluidic technique, gas sensor, etc.

Marvin D. Shaw is a research scientist at the National Centre for Atmospheric Science in the Wolfson Atmospheric Chemistry Laboratories, Department of Chemistry, University of York, UK. He obtained his Ph. D. from the University of York in 2011.

Alastair C. Lewis is a science director at the National Centre for Atmospheric Science, UK, and the professor of atmospheric chemistry at the University of York, UK.

Lucy J. Carpenter is the professor of atmospheric chemistry at the University of York, UK. Her research interests include the chemistry occurring in atmosphere-ocean interactions, impact of oceanic emissions on atmospheric oxidation and climate.

Tanya Batchellier is an undergraduate in the Department of Chemistry, University of York, UK. She will graduate in 2017.